3.3.2 LTSK1

Atmospheric Correction and Reflectance Algorithm

A. Algorithm Outline

(1) Algorithm Code: LTSK 1

(2) Product Code: ACLC

(3) PI names: G18 Dr. Alfredo Huete

(4) Overview of algorithm (Standard level)

Algorithm objectives

The algorithm has the following objective:

To atmospherically correct the composited, normalized radiances for "Rayleigh scattering and ozone absorption" on a per-pixel basis.

B. Theoretical Description

(1) Methodology and Logic Flow

A general flowchart describing atmosphere correction is presented in figure 1. Atmospheric correction is performed after the temporal mosaicking to reduce processing loads and disk space as only one image is processed every composite period (16-day). Rayleigh scattering and ozone absorption are corrected with the assistance of ancillary data provided by GAIT, such as the TOVS data set and GTOPO30. Much of the computation during atmospheric correction requires intensive CPU time due to floating point processing.

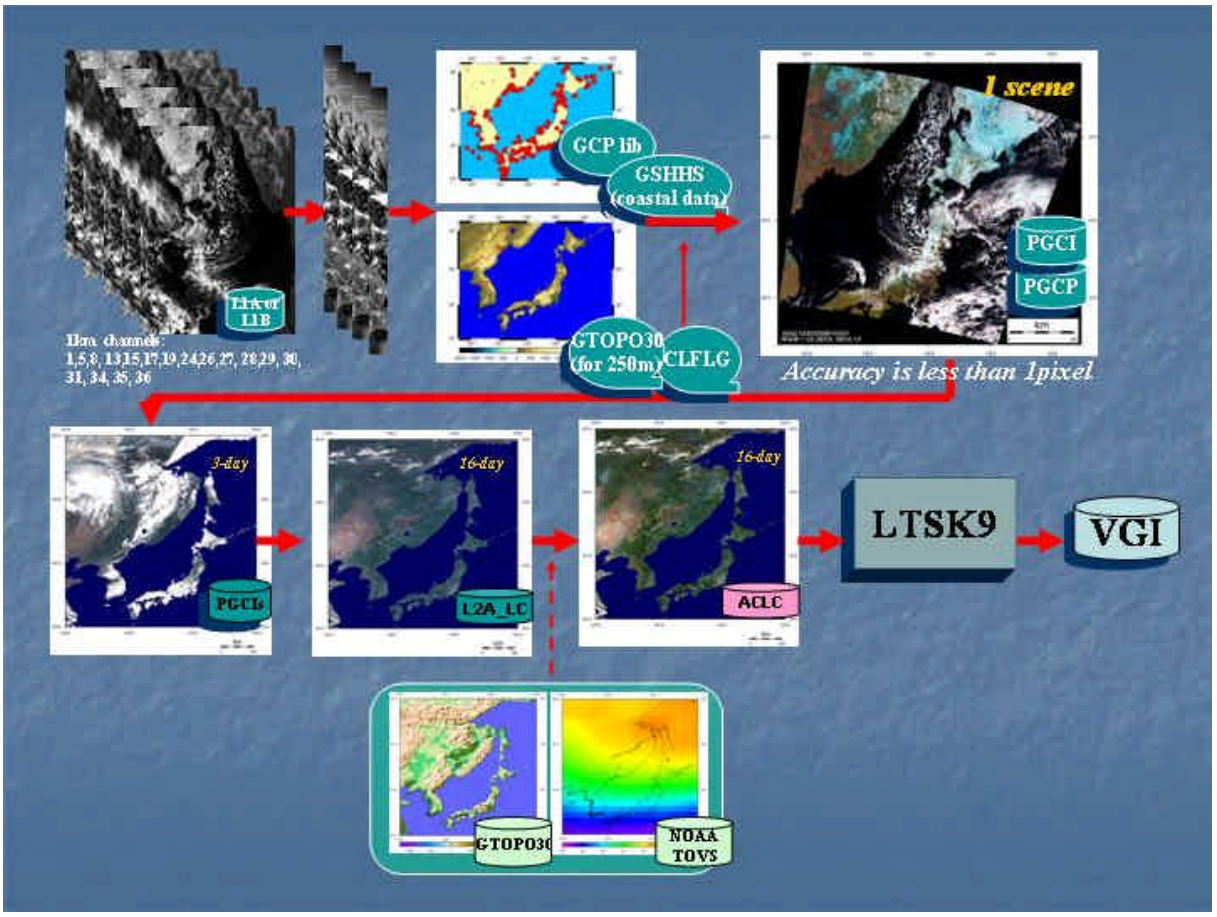

Figure 1: Flow diagram for the Atmospheric Correction and Reflectance Algorithm(LTSK1).

(2) Physical and Mathematical Aspects of the Algorithms

Atmospheric Radiative Transfer Modeling Algorithm

GLI atmospheric correction for land is conducted for Rayleigh scattering and Ozone absorption. Much of the computation during atmospheric correction requires intensive CPU time due to floating point processing. Therefore, this algorithm is adopted methodology by using Look-Up tables (LUTs). GLI land atmospheric correction has some assumptions as the following items.

* Ozone layers are above molecular layer

* All molecules are above aerosols

* System of (aerosol layer + ground surface) is assumed as Lambertian

* Horizontally homogeneous

Rayleigh scattering and ozone absorption are corrected with the assistance of ancillary data NOAA/TOVS data set and GTOPO30. GLI observed reflectance at Top-Of-Atmosphere is described as the following equation:

$$\rho_{obs}(\tau_{O_3},\tau_R,\theta_s,\theta_v,\varphi_{s-v}) = T_{O_3}(\tau_{O_3},\theta_s,\theta_v) \times (\rho_R(\tau_R,\theta_s,\theta_v,\varphi_{s-v}) + \frac{T_{R\downarrow}(\tau_R,\theta_s)\rho_s T_{R\uparrow}(\tau_r,\theta_v)}{1 - S_R(\tau_R)\rho_s})$$

where ρ_{obs} is GLI observed reflectance derived from composite algorithm, T_{O_3} is ozone transmittance, ρ_R is path radiance, $T_{R\downarrow}$ is downward transmittance, $T_{R\uparrow}$ is upward transmittance, S_R is spherical albedo, and ρ_s is Rayliegh/Ozone corrected reflectance, which is output of this algorithm. The path radiance, upward and downward transmittance and spherical albedo were tabulated as functions of optical thickness of Rayleigh scattering (τ_R), view and illumination angles. Then, these four values will be retrieved based on the values of τ_R for each pixel at each land channel based on the pixel elevation, BPF, and STSG (Sun-Target-Sensor Geometry). τ_R relates to elevation through standard pressure and temperature (US62), which can be calculated with GTOPO30. And T_{O_3} can be derived from NOAA/TOVS data.

(2) Calibration and Validation

(3) Quality Control and Diagnostic Information:

The algorithm will include a portion dealing with Quality Assurance (QA) issues. The goal of the QA is to guarantee a better data quality and consistency both spatially and temporally. Inconsistent products may depict spatial and temporal variations in their values unrelated to Earth's surface states and processes. In order to prevent such data consistency problems and poor data quality of that kind, it is necessary to develop such an algorithm. The GLI atmospheric correction will have a built-in QA/QC routine to warrant the data quality. figure 15 shows an example of such a QA/QC product.

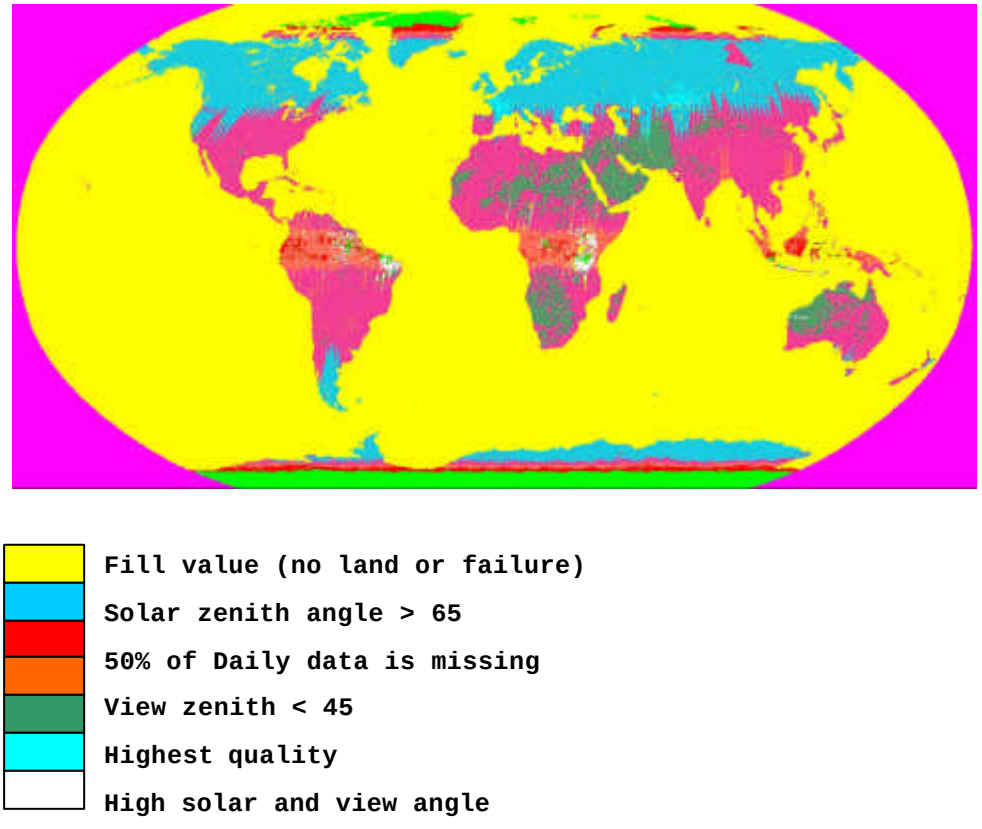

Figure 15: Example of QA/QC map for GLI

(4) Exception Handling

Exception handling is the technique adopted to account for unforeseen situations. Missing data, missing ancillary data, sensor behavior, floating point error during computation, data out of range and so on. In a generic approach, any time the algorithm does not perform as designed, the data will generate an exception handler. However, during the run the algorithm will use a generic success flag to track the execution of the different parts. Anytime an exception handler is generated the pixel value will not be updated (VI's case) and most probably a pre-determined value (-300, -2000) will be appended instead. When the atmospheric correction algorithm fails a scheme was designed that consists of using a set of fill values generated before the compositing takes place.

(5) Constraints, Limitations, Assumptions

As proposed in phase one, the atmospheric correction will only be concerned with Rayleigh and Ozone. Three major shortcomings are noted here:

1) No account for BRDF

2) No account for aerosol over land

2) Not account for water vapor

For the time being we advise that aerosol correction should be applied at a later stage and on a per demand basis. The BRDF product, by which data will be normalized to "*nadir*" view angles could be adopted if research, and funding permits.

(6) Suggestions and Recommendations

We will be looking into the feasibility, should the need arise, of extending the radiative transfer methods described in this ATBD in order to potentially accommodate calculations of aerosol scattering (based plausibly upon current climatological models of tropospheric and stratospheric haze geographic and altitudinal distributions) and water vapor absorption in the visible and near-IR. Incorporation of the latter effect into our present code would follow the lines we have discussed regarding our treatment of ozone discussed elsewhere in this report. A full-fledged treatment on a global scale of the extinction of sunlight by small airborne particles is of course tremendously more difficult to achieve. It's important to realize at this stage, that correction for aerosol is being applied by the ocean group, and we are identifying means of coordinating our work. The data flow-diagram proposed by GAIT and limitations in resources will make some of these tasks hard to apply. Overall, we are confident in the current status of our research, and hope to extend the GLI contribution to the remote sensing community by devising better and sounder techniques for data production.

D. References

Ackerman, S., K. Strabala, P. Menzel1, R. Frey, C. Moeller, L. Gumley, B. Baum, C. Schaaf, G. Riggs, R. Welch, 1996. Discriminating Clear-sky from Cloud with Modis Algorithm Theoretical Basis Document V3, http://eospso.gsfc.nasa.gov/atbd/modistables. html.

Agbu, P.A., and James, M.E., 1994. The NOAA/NASA Pathfinder AVHRR Land Data Set User's Manual. Goddard Distributed Active Archive Center, NASA, Goddard Space Flight Center, Greenbelt.

Asano, S. and Uchiyama, A. (1987), Application of an extended ESFT method to calculation of solar heating rates by water vapor absorption, J.Quant. Spectrosc. Radiat. Transfer, 38. 147-158.

Asrar, G., Fuchs, M., Kanemasu, E.T. and Hatfield, J.L., 1984, Estimating absorbed photosynthetic radiation and leaf area index from spectral reflectance in wheat, Agron. J., 76:300—306.

Asrar, G., Myneni, R.B., and Choudhury, B.J., 1992, Spatial heterogeneity in vegetation canopies and remote sensing of absorbed photosynthetically active radiation: a modeling study. Remote Sens. Environ. 41:85-101.

Baret, F., and Guyot, G., 1991. Potentials and limits of vegetation indices for LAI and APAR assessment. Remote Sens. Environ. 35: 161-173.

Bohren, C.F. and Huffman,D.R. (1983), Absorption and Scattering of Light by Small Particles, Wiley-Interscience, New York.

Chandrasekhar, S. (1960), Radiative Transfer, Dover, New York.Coulson, K.L., (1988) Polarization and Intensity of Light in the Atmosphere, A. Deepak, Hampton, Virginia.

Choudhury, B.J., 1987, Relationships between vegetation indices, radiation absorption, and net photosynthesis evaluated by a sensitivity analysis, Remote Sens. Environ. 22:209-233.

Cihlar, J., Manak, D., and D'Iorio, M., 1994b. Evaluation of Compositing Algorithms for AVHRR Data over Land. IEEE Trans. Geosc. Remote Sens., 32:427-437.

Cihlar, J., Manak, D., and Voisin, N., 1994a. AVHRR Bidirectional Reflectance Effects and Compositing. Remote Sens. Environ., 48:77-88

Cihlar, J.C., H. Ly, Z. Li, J. Chen, H. Pokrant, and F. Huang, 1997. Multitemporal, Multichannel AVHRR data sets for Land Biosphere Studies— Artifacts and Corrections. Remote Sens. Environ. 60:35-57.

Deering, D.W. and Eck, T.E., 1987. Atmospheric optical depth effects on angular anisotropy of plant canopy reflectance. Int. J. Remote Sensing, 8(6), 893-916.

Deering, D.W. and Leone, 1986. A sphere-scanning radiometer for rapid directional measurements of sky and ground radiance, Remote Sens. Environ., 19:1-24.

Eidenshink, J.C. and Faundeen, J.L., 1994, "The 1km AVHRR global land data set: first stages in implementation," Int. J. Remote Sensing, 15(17), pp. 3443-3462.

Fung, Y., Tucker, C.J. and Prentice, K.C., 1987. Application of Advanced Very High Resolution Radiometer Vegetation Index to Study Atmosphere-Biosphere Exchange of CO_2. J. Geoph. Res., 92, 2999-3015.

Giver, L.P., Benner, D.C., Tomasko, M.G., Fink, U. and Kerola, D.X.(1990), Gaussian quadrature exponential sum modeling of near infrared methane laboratory spectra obtained at temperatures from 106 to 297 K.,in First International Conference on Laboratory Research for Planetary Atmospheres, pp. 147-156. NASA CP 3077.

Goody, R.M. and Yung, Y.L. (1989), Atmospheric Radiation: Theoretical Basis, Second Edition, Oxford University Press, New York.

Gordon, H.R., Brown, J.W., and Evans, R. H. (1988), Exact Rayleigh scattering calculations for use with the Nimbus-7 Coastal Zone Color Scanner, Applied Optics, **27**, 862-871.

Goward, D.G., Turner, S., Dye, D.G., and Liang, J., 1994. University of Maryland improved Global Vegetation Index. Int. J. Remote Sensing, 15(17), 3365-3395.

Goward, S.N. Dye, D.G., Turner, S., and Yang, J., 1993. Objective assessment of the NOAA global vegetation index data product. Int. J. Remote Sensing, 14, 3365-3394.

Goward, S.N., and Huemmrich, K.F., 1992, Vegetation canopy PAR absorptance and the normalized difference vegetation index: an assessment using the SAIL model, Remote Sens. Environ. 39:119-140.

Goward, S.N., B. Markham, D.G. Dye, W. Dulaney, J. Yang, 1991, "Normalized difference vegetation index measurements from the Advanced Very High Resolution Radiometer", Remote Sens. Environ., 35:257-277.

Gutman, G.G., 1991, Vegetation indices from AVHRR: an update and future prospect, Remote Sens. Environ., 35:121-136._

Hansen, J.E. (1971), Multiple scattering of polarized light in planetary atmospheres. Part II. Sunlight reflected by terrestrial water clouds, J. Atmos. Sci., 28, 1400-1426.

Hansen, J.E. and Travis, L.D. (1974), Light scattering in planetary atmospheres, Space Sci. Rev., 16, 527-610.

Herman, B.M. and Browning, S.R. (1965), A numerical solution to the equation of radiative transfer, J. Atmos. Sci., 22, 559-566.

Holben, B.N. 1986. Characterization of maximum value composites from temporal AVHRR data. Int. J. Remote Sensing, 7:1417-1434.

Huete, A.R. ,1988, A soil adjusted vegetation index (SAVI), Remote Sens. Environ. 25:295-309.

Huete, A.R., Justice, C.O., van Leeuwen, W.J.D., 1996. "MODIS vegetation Index, Algorithm Theoretical Basis Document," http://eospso.gsfc.nasa.gov/atbd/modistables. html.

Huete, A.R., Liu, H.Q., Batchily, K., and van Leeuwen, W., 1997, A comparison of vegetation indices over a global set of TM images for EOS-MODIS, Remote Sens. Environ., 59:440-451.

Iqbal, M. (1983), Introduction to Solar Radiation, Academic Press, New York.

James, M.D., and Kalluri, S.N.V. (1994), The Pathfinder AVHRR land data set: An improved coarse resolution data set for terrestrial monitoring, Int. J. Remote Sensing, 15(17):3347-3363.

Justice, C.O., Townshend, J.R.G., Holben, B.N. and Tucker, C.J.,1985, "Analysis of the phenology of global vegetation using meteorological satellite data", Int. J. Remote Sensing, 6:1271-1318.

Kaufman, Y.J. and Tanré, D., 1992, Atmospherically resistant vegetation index (ARVI) for EOS-MODIS, IEEE Trans. Geosci. Remote Sensing, 30:261-270.

Kerola, D. X. (1994), Near-Infrared Spectroscopic Studies of the Troposphere of Saturn, Ph.D. Dissertation The University of Arizona.

Kerola, D. X. (1996), Polarizatio n and intensity of sunlight in the Earth's atmosphere: revisiting the Gauss-Seidel modeling approach, Bull. Amer. Astron. Soc., 28, 1158.

Kerola, D. X., Larson, H. P ., and Tomasko, M. G. (1997), Analysis of the near-IR spectrum of Saturn: a comprehensive radiative transfer model of its middle and upper troposphere, Icarus, 127, 190-212.

Kimes, D.S., Holben, B.N., Tucker, C.J., and Newcomb, W.W., 1984. Optimal directional view angles for remote-sensing missions. Int. J. Remote Sensing 5(6), 887-908.

Kimes, D.S., Newcomb, N.W., Tucker, C.J., Zonneveld, I.S., Van Wijngaar-den, W. De Leeuw, J. and Epema, G.F.(1985), Directional reflectance factor distributions for cover types of northern Africa, Remote Sens. Environ., 17, 1-19.

Kimes, D.S., Newcomb, W.W., Tucke r, C.J., Zonneveld, I.S., Van Wijngaarden, W., De Leeuw, J., and Epema, G.F., 1985. Directional Reflectance Factor Distribution for Cover Types of Northern Africa. Remote Sens. Environ. 18:1-19.

Kuchler, A.W., 1995. Natural vegetation map, In: Rand McNally Goode's World Atlas; 19th edition. Eds. Espenshade E.B. Hudson, J.C., Morrison, J.L.. p 18-19.

Lacis, A. (1990), private communication. Leckner, B. (1978), The spectral distribution of solar radiation at the earth's surface - elements of a model, Solar Energy, 20(2), 143-150.

Leeuwen van, W.J.D. A.R. Huete, S. Jia, C.L Walthall, 1996. Comparison of Vegetation Index Compositing Scenarios: BRDF Versus Maximum VI Approaches. IEEE- IGARSS'96, Lincoln Nebraska, Vol.3, 1423-1425.

Leeuwen van, W.J.D., A.R. Huete, J. Duncan, J. Franklin, 1994. Radiative transfer in shrub savanna sites in Niger -- preliminary results from HAPEX-II-Sahel: 3. Optical dynamics and vegetation index sensitivity to biomass and plant cover. Agricultural and Forest Meteorology 69, 267-288.

Leeuwen van, W.J.D., A.R. Huete., K. Didan and T. Laing, 1997a. Modeling bi-directional reflectance factors for different land cover types and surface components to standardize vegetation indices. 7th Int. Symp. Phys. Measurements and Signatures in Remote Sensing, Courcheval. (pp 1-8; in press)

Leeuwen van, W.J.D., Trevor W. Laing, and Alfredo R. Huete, 1997b. Quality Assurance of Global Vegetation Index Compositing Algorithms Using AVHRR Data. IEEE- IGARSS'97, Singapore (pp 1-3; in press)

Liou, K.N. (1980), An Introduction to Atmospheric Radiation, Academic Press, San Diego.

Liu, H.Q., and Huete, A.R., 1995, "A feedback based modification of the NDVI to minimize canopy background and atmospheric noise", IEEE Trans. Geosci. Remote Sensing, 33:457-465.

Marchuk, G.I. (1980), The Monte Carlo Methods in Atmospheric Optics, Springer-Verrlag, New York.

Mercer, R.D., Dunkelman, L., Shaw, G. E., Larson, S. M. and Kerola, D. X. (1997), Solar spectral radiance measurements: connectivity across time and place, Proceedings of the NEWRAD'97 conference, held in Tucson, Arizona, October 27-29, 1997.

Meyer, D., Verstraete, M. and Pinty, B., 1995. The effect of surface anisotropy and viewing geometry on the estimation of NDVI from AVHRR. Remote Sensing Reviews, 12:3-27.

Miura T., A. Huete, van Leeuwen. W.J.D., K. Didan, 1997. Vegetation Detection Through Smoke Filled AVIRIS images: An assessment using MODIS band passes. J. Geoph. Res.. Submitted

Moody, A. and Strahler, A.H., 1994, Characteristics of composited AVHRR data and problems in their classification. Int. J. Remote Sensing, 15(17), 3473-3491.

Myneni, R.B. and Asrar, G., 1993, Atmospheric effects and spectral vegetation indices, Remote Sens. Environ.

Myneni, R.B., Hall, F.G., Sellers, P.J., and Marshak, A.L., 1995, "The interpretation of spectral vegetation indices", IEEE Trans. Geosci. Remote Sens.

Nemani, R., Pierce, L., Running, S., and Band, L., 1993. Forest ecosystem processes at the watershed scale: sensitivity to remotely-sensed Leaf Area Index estimates. Int. J. Remote Sens. 14(13): 2519-2534.

Price, J.C., 1987. Calibration of Satellite Radiometers and the Comparison of Vegetation Indices. Rem. Sensing Environ., 21:419-422.

Prince, S.D., 1991, A model of regional primary production for use with coarse resolution satellite data. International Journal of Remote Sensing, 12(6):1313-1330.

Privette, J.L. Myneni, R.B., Emery, W.J. and Hall, F.G., 1996a. Optimal sampling conditions for estimating grassland parameters via reflectance model inversions. IEEE Trans. Geosci. Remote Sens. Vol. 34(1):272-284.

Privette, J.L., Deering, D.W., and Eck, T.E., 1996b. Estimating albedo and nadir reflectance through inversion of simple BRDF models with AVHRR/MODIS-like data. J. Geoph. Res. BOREAS special issue, submitted.

Qi, J. and Kerr, Y., 1997. On Current Compositing Algorithms. Remote Sensing Reviews, 15:235-256.

Qi, J., Huete, A.R., Hood, J., and Kerr, Y., 1994c. Compositing Multi-temporal remote sensing data sets. PECORA 11, Symposium on land information systems, Sioux Falls August 1993. p. 206-213.

Rahman, H., Pinty, B. and Verstraete, M.M., 1993. Coupled surface-atmosphere reflectance (CSAR) model 2. Semi-empirical surface model usable with NOAA AVHRR. J. Geophys. Res. 89(D11):20791-20801.

Raich, J.W., and Schlesinger, W.H., 1992, The global carbon dioxide flux in soil respiration and its relationship to vegetation and climate, Tellus 44B:81-99.

Roujean, J.L., Leroy, M., Podaire, A., and Deschamps, P.Y., 1992. Evidence of surface reflectance bidirectional effects from a NOAA/AVHRR multi-temporal data set. Int. J. Remote Sensing 13(4), 685-698.

Roy, D.P., 1997. Investigation of the maximum normalized difference Vegetation Index (NDVI) and the Maximum surface temperature (T_s) AVHRR compositing procedures for the extraction of NDVI and Ts over forest. Int. J. Remote Sens. 18(11):2383-2401.

Running, S.W., and Nemani, R.R, 1988, Relating seasonal patterns of the AVHRR vegetation index to simulated photosynthesis and transpiration of forest in different climates, Remote Sens. Environ. 24:347-367.

Running, S.W., Justice, C., Salomonson, V., Hall, D., Barker, J., Kaufmann, Y., Strahler, A., Huete, A., Muller, J.P., VanderBilt, V.,Wan, Z.M., Teillet, P. and Carneggie, D., 1994. Terrestrial Remote Sensing Science and Algorithms planned for EOS/MODIS. Int. J. Remote Sensing, Vol. 15, 17:3587-3620.

Salomonson, V.V., Barnes, W.L., Maymon, P.W., Montgomery, H.E. and Ostrow, H., 1989, MODIS: advanced facility instrument for studies of the earth as a system, IEEE Trans. Geosci. Remote Sens. 27:145-153.

Sellers, P.C. , 1985, Canopy Reflectance, photosynthesis and transpiration, Int. J. Remote Sens. 6:1335-1372

Sellers, P.J., Tucker, C.J., Collatz, G.J., Los S., Justice, C.O., Dazlich, D.A., and Randall, D.A., 1994, "A global 1° * 1° NDVI data set for climate studies. Part 2 - The adjustment of the NDVI and generation of global fields of terrestrial biophysical parameters", Int. J. Remote Sensing, 15:3519-3545.

Stowe, L.L., E.P. McClain, R. Carey, P. Pellegrino, G.G. Gutman, P. Davis, C. Long, and S. Hart. 1991. Global distribution of cloud cover derived from NOAA/AVHRR operational satellite data. Advances in Space Research, 3:51-54.

Strahler, A, et al., 1996. MODIS BRDF/Albedo Product : ATBD version 4. http://eospso.gsfc.nasa.gov/atbd/modistables. html.

Tans, P.P., Fung, I.Y., and Takahashi, T. (1990), Observational constraints on the global atmosphere CO2 budget. Science 247:1431-1438.

Teillet, P.M., Staenz, K., and Willams, D.J., 1997. Effects of Spectral, Spatial , and Radiometric Characteristics on Remote Sensing Vegetation Indices of Forested Regions. Remote Sens. Environ. 61:139-149.

Thome, K.J., Gellman, D.I., Parada, R.J., Biggar, S.F., Slater, P.N., and Moran, M.S. (1993), In-flight radiometric calibration of Landsat-5 Thematic Mapper from 1984 to present, in Proceedings of SPIE, vol. 1938, 126-130.

Tomasko, M.G. and Doose, L.R. (1989), private communication.

Townshend, J.R.G., 1994, Global data sets for land applications from the AVHRR: an introduction. Int. J. Remote Sensing, 15:3319-3332.

Townshend, J.R.G., C. Justice, W. Li, C. Gurney, and J. McManus, 1991, "Global land cover classification by remote sensing: present capabilities and future possibilities", Remote Sens. Environ., 35:243-256.

Townshend, J.R.G., Justice, C.O., Gurney, C. and McManus, J., 1992, The impact of misregistration on the detection of changes in land cover, IEEE Trans. Geosci. Remote Sens., 30(5):1054-1060.

Tucker, C.J. and Sellers, P.J., 1986, Satellite remote sensing of primary productivity, International Journal of Remote Sensing, 7:1395-1416.

Vermote, E., Remer, L.A., Justice, C.O., Kaufman, Y.J., and Tanré, 1995, ATBD Atmosphere correction algorithm: Spectral reflectances (MOD09), Version 2.

Vermote, E., Tanré, D., Deuzé, J.L., Herman, M., and Mocrette, J.J., 1997, Second Simulation of the Satellite Signal in the Solar Spectrum: an overview. IEEE Trans. Geosc. Remote Sens., 35(3):675-686.

Vermote, E.F., Tanre, D., Deuze, J.L., Herman, M. and Morcrette, JJ. (1997), Second simulation of the satellite signal in the solar spectrum, 6S: an overview, IEEE Transactions on Geoscience and Remote Sensing, 35, No. 3, 675-686.

Vierling, L.A., Deering, D.W., Eck, T.F., 1997. Differences in Arctic Tundra Vegetation Type and Phenology as Seen Using Bidirectional Radiometry in the Ea rly Growing Season. Remote Sens. Environ. 60:71-82.

Viovy, N., Arino, O. and Belward, A.S., 1992. The best index slope extraction (BISE): A method for reducing noise in NDVI time series. Int. J. Rem. Sensing, Vol:13, 8:1585-1590.

Walter-Shea, E.A., Privette, J., Cornell, D., Mesarch, M.A., Hays, C.J., 1997, Relationship between directional spectral vegetation indices and leaf area and absorbed radiation in alfalfa. Remote Sens. Environ. (In press)

Walthall, C.L., Norman, J.M., Welles, J.M., Campbell, G., and Blad, B.L., 1985, Simple equation to approximate the bi-directional reflectance from vegetative canopies and bare soil surfaces," Applied Optics, 24(3), pp. 383-387.

Wanner W., A.H. Strahler, B. Hu, P. Lewis, J.-P. Muller, X.. Li, C.L. Barker Schaaf, and M.J. Barnsley, 1997. Global retrieval of bidirectional reflectance and albedo over land from EOS MODIS and MISR data: Theory and algorithm. J. Geoph. Res., 102, D14, 17143-17161.

Wanner W., X.. Li, A.H. Strahler, 1995. On the Derivation of kernel-driven models of bidirectional reflectance. J. Geoph. Res., 100, D10, 21077-21089

Wolfe. R., D. Roy. Georegistration of MODIS data (level 2G), to be submitted

Wu, A., Li, Z. and Cihlar, 1995, Effects of land cover type and greenness on advanced very high resolution radiometer bidirectional reflectances: Analysis and removal. J. Geophys. Res., 100(D5), 9179-9192.

E. APPENDIX 1

Summary of the ESFT Technique: Application to CH4 Absorption in Saturn for the λ = 1.7 - 2.6 μm Spectral Region

The "exponential-sum-fitting of transmittances" (ESFT) technique has been in general use for some time as a numerical means for evaluating absorption coefficients for a variety of molecular species. The ESFT method is especially attractive for use in the determination of effective absorption coefficients for gases in planetary atmospheres where the multiple scattering of light by haze and cloud aerosols is important. A host of "band-model" formulations for calculating the transmittance of sunlight through layers of "clean" gas abound. Such parameterization of line strength and line spacing for complex absorption bands like those exhibited by CH_4 and H_2O is quite satisfactory for traditional RLM studies of planetary atmospheres. But as soon as small particles are envisaged to be mixed-in with the gaseous constituents, band-model representations of spectral line optical depths are rendered intractable for use in scattering models.

The underlying rationale for adopting the ESFT approach is as follows: because there is no correlation whatsoever between the magnitude of the absorption coefficient and the frequency of the radiation, a transformation can be made from k(ν) to k(u), i.e., the absorption coefficient as a function of frequency can be recast as an "effective" absorption coefficient, k_{eff}, which is a function of the optical path u. The transmittance is:

$$T(u) = (\Delta u)^{-1} \int \exp(-k_\nu u) du$$

The ESFT methodology is not too dissimilar from an approach known as the "k-distribution". As Goody and Yung (1989) point out, it is sufficient to know what fraction f(k)dk of the frequency domain ν can be represented by absorption coefficients between k and k + dk. No importance is attached to the location in frequency space of a given value of k. An expression entirely is:

$$T(u) = \int f(k) \exp(-ku) dk$$

where f(k)dk is the k-distribution function. It is readily recognizable that f(k) is the inverse Laplace transform of T(u).

The ESFT approach circumvents the necessity of evaluating the inverse Laplace transform. ESFT is inherently a numerical analysis problem, and as such it is intrinsically ill-conditioned. The specific set of algorithms we used to determine the effective CH_4 k's, originated with Asano and Uchiyama (1987). They have extended the traditional ESFT technique to incorporate an iterative non-linear least squares fitting of an ordered set of the effective k's. The work of Asano and Uchiyama represents an improvement in a real, practical sense over many previous implementations of the ESFT technique. Their approach relies on the pre-selection of a set of weights, w_i , such that

$$T(u) \cong \sum w_i \exp(-k_i u)$$

These weights can be quite accurately determined once a preferred quadrature scheme is adopted. The heart of the Asano and Uchiyama ESFT procedure is the successive correction of the k_i 's for the set of fixed w_i 's. The virtue of this extended ESFT technique is its ability to find a best-fitting set of k_i 's for a wide range of absorber amounts, u, which might not necessarily be equally spaced.

Kerola (1989, private contributions) developed the FORTRAN code. It was implemented in conjunction with Tomasko for modeling CH_4 absorptions in Titan's near-IR and visible spectrum. The program was structured in a fashion to permit direct assessment of the standard deviation of the transmittances computed via ESFT versus those obtained from wide-band laboratory measurements of transmittances made at NASA Ames Research Center. The Ames laboratory data was generated by Giver (1990). Best-fit values for a monochromatic absorption coefficient, k_ν , and a pressure coefficient, y_ν , were obtained by Giver from comparison of his experimental data to that given in the Malkmus random-band model. The transmittance in the Malkmus model is:

$$T_M = \exp\left(-2py_\nu p\left(\left[\frac{k_\nu u}{py_\nu p} + 1 \right]^{1/2} - 1 \right) \right)$$

The pressure parameter, y_ν, is the ratio of the line width at 1 atmosphere to the mean line spacing. It has units of atm $^{-1}$. The atmospheric pressure is p (in atm). The Ames measurements were made at 3 temperatures: T= 112 K, 188 K, and 295 K. The full Ames dataset extends from about 3770 cm $^{-1}$ to close to 9000 cm $^{-1}$. The spectral transmittances are recorded at every 10 cm $^{-1}$. In

our Saturn modeling (Kerola, 1994), we performed the exponential-sum fitting on spectral intervals 50 cm^{-1} wide, spanning the region 3785 - 5995 cm^{-1} Our efforts included only the low and mid-temperature Ames datasets. We used a linear extrapolation of the k_i 's over temperature. For most of the CH_4 bands, the effective levels probed in Saturn's troposphere are slightly colder than about 100 K.

As a matter of computational ease and accuracy, the ESFT code was designed to use 8-point Gaussian quadrature for the determination of the weights. The most important final output of the program is a set of 8 best-fit ESFT k's. These "equivalent" absorption coefficients are arranged so that they are in ascending order (i.e, $k_1 < k_2 < k_3$, etc). 8 k_i values are generated for each spectral interval ($\Delta\nu$ = 50 cm^{-1}), and for each atmospheric pressure p. For each spectral interval, $T_M(u_i)$ is computed using equal spacing in the logarithm of absorber amount. The initial guess for the absorption coefficient is given by:

$$k_i^{(0)} = \frac{\ln T_i}{u_i}$$

60 values of u_i were calculated. Two conditions of convergence involve either iterating at most 100 times or ending the iterations when the relative RMS. error is less than 0.2 percent. Convergence is often quite rapid, taking typically less than a couple dozen iterations for most spectral bands, and for most pressures.